Am J Cancer Res 2023;13(10):4721-4733
www.ajcr.us /ISSN:2156-6976/ajcr0151363

Original Article

Inhibition of Na+/H+ exchanger (NHE) 7 by 5-(N-ethyl-N-isopropyl)-Amiloride displays anti-cancer activity in non-small cell lung cancer by disrupting cancer stem cell activity and downregulating PD-L1 expression

Bing-Yen Wang[1,2*], Huan-Ting Shen[3*], Yu-Ling Lee[4], Peng-Ju Chien[4], Wen-Wei Chang[4,5]

[1]Division of Thoracic Surgery, Department of Surgery, Changhua Christian Hospital, No. 135, Nanhsiao Street, Changhua 500209, Taiwan; [2]Department of Post-Baccalaureate Medicine, College of Medicine, National Chung Hsing University, No. 145, Xingda Rd., South Dist., Taichung 402202, Taiwan; [3]Department of Pulmonary Medicine, Taichung Tzu Chi Hospital, Buddhist Tzu Chi Medical Foundation, No. 88, Sec. 1, Fengxing Rd., Tanzi Dist., Taichung 427, Taiwan; [4]Department of Biomedical Sciences, Chung Shan Medical University, No. 110, Sec. 1, Jianguo N. Rd., Taichung 402306, Taiwan; [5]Department of Medical Research, Chung Shan Medical University Hospital, No. 110, Sec. 1, Jianguo N. Rd., Taichung 402306, Taiwan. [*]Equal contributors.

Received May 22, 2023; Accepted August 6, 2023; Epub October 15, 2023; Published October 30, 2023

Abstract: The alkaline intracellular environment of cancer cells is critical for cell proliferation and controlled by various plasma membrane transporters including Na+/H+ exchangers (NHEs). NHEs can also mediate cell behavior by regulating signaling transduction. In this study, we investigated the role of NHE7 in cancer stem cell (CSC) activity in non-small cell lung cancer (NSCLC) cells and the potential therapeutic implications of targeting NHE7 and the associated immune checkpoint molecule PD-L1. By analyzing the database from The Cancer Genome Atlas, we found a positive correlation between *SLC9A7* mRNA levels (the gene encoding NHE7) and poor overall survival in lung adenocarcinoma patients. Using 5-(N-ethyl-N-isopropyl)-Amiloride (EIPA) to inhibit NHE7 activity, we observed disrupted cell cycle progression and suppressed NSCLC cell proliferation without inducing apoptosis. Furthermore, EIPA demonstrated a suppressive effect on CSC activity, evidenced by decreased tumorsphere numbers and inhibition of CSC markers such as ALDH1A2, ABCG2, CD44, and CD133. Flow cytometric analysis revealed that EIPA treatment or NHE7 knockdown in NSCLC cells led to downregulated PD-L1 expression, associated with inhibited STAT3 activity. Interestingly, EIPA's CSC-targeting activity was preferentially observed in NSCLC cells overexpressing BMI1, while increased PD-L1 expression was detected in BMI1-overexpressing NSCLC cells. Our findings suggest that targeting NHE7 with inhibitors like EIPA may have therapeutic potential in NSCLC treatment by disrupting cell cycle progression and suppressing CSC activity. The observed increase in PD-L1 expression in BMI1-overexpressing NSCLC cells upon EIPA treatment highlights the potential benefit of combining NHE7 inhibitors with anti-PD-L1 agents as a promising new therapeutic strategy for NSCLC.

Keywords: Na+/H+ exchanger 7, EIPA, cancer stem cells, PD-L1, non-small cell lung cancer, STAT3

Introduction

Lung cancer is the leading cause of cancer-related death globally; it is responsible for 18% of all cancer deaths [1]. Based on histological examination, it can be broadly classified into two main types: small cell lung cancer (SCLC) and non-small cell lung cancer (NSCLC). NSCLC is the more common type, with adenocarcinoma accounting for approximately 40% of cases [2]. Unfortunately, a significant proportion of NSCLC patients (around 40%) are diagnosed at an advanced stage, with a five-year overall survival rate of less than 10% [3, 4]. In addition to conventional treatments, therapeutic antibodies targeting programmed cell death 1 (PD-1), such as Nivolumab or Pembrolizumab, or programmed cell death ligand 1 (PD-L1), such as

Atezolizumab, have been approved as second-line drugs for advanced NSCLC [4]. However, the response rates to anti-PD-1/anti-PD-L1 therapy are modest, with a best-case scenario of 47%-63% [5]. This suggests that NSCLC patients exhibit primary resistance to anti-PD-1/anti-PD-L1 therapy. In addition to its immune suppressive activity, PD-L1 expression on tumor cells has been shown to contribute to malignant features by inducing drug resistance in myeloma cells [6] and reducing interferon-induced apoptosis [7]. Our previous research has revealed that knockdown of PD-L1 in NSCLC cells resulted in decreased cancer stem cell (CSC) activity [8], a malignant feature that is crucial for tumor initiation, drug resistance, and metastasis [9]. Therefore, PD-L1 expression on tumor cells not only transmits immunosuppression in the tumor microenvironment but also contributes to the malignant phenotypes of tumor cells themselves. Understanding the regulation of PD-L1 expression on tumor cells could lead to new insights for drug development.

Metabolic alterations are a hallmark of cancer cells, with the Warburg effect being a well-established phenomenon in which cancer cells exhibit aerobic glycolysis and produce lactate to lower extracellular pH [10]. In turn, intracellular pH reduction can trigger apoptosis or growth inhibition in cancer cells, as pH influences cell proliferation. A pH greater than 7.2 is known to be a threshold for growth factor-induced transition from the G1 phase to the S phase [11]. To increase cytosolic pH, cancer cells enhance the expression or activity of membrane proton transporters or pH regulators, such as Na+/H+ exchangers (NHEs), carbonic anhydrases, monocarboxylate transporters 1 and 4, and Na+-driven HCO3- exchangers [12]. NHE7 (gene symbol *SLC9A7*) is a Na+/H+ antiporter located on the endosome membrane, which transports protons from the cytoplasm to the endosome to increase cytosolic pH [13]. In MDA-MB-231 breast cancer cells, NHE7 was shown to associate with actin/vimentin/CD44 via protein-protein interactions, suggesting a potential role for NHE7 in the epithelial-mesenchymal transition (EMT) process in cancer cells [14]. Onishi et al. demonstrated that NHE7 overexpression in MDA-MB-231 cells promoted cell proliferation and invasiveness in vitro and in vivo [15]. Moreover, Galenkamp et al. recently reported that high NHE7 expression strongly correlates with poor overall survival in pancreatic adenocarcinoma patients. Knockdown of NHE7 suppressed cell proliferation and induced cell death in pancreatic adenocarcinoma cells [16]. However, the role of NHE7 in non-small cell lung cancers remains unclear, despite its reported positive effects on cell proliferation and invasiveness in some cancer types. The present study aimed to investigate the role of NHE7, encoded by the *SLC9A7* gene, in NSCLC and its potential as a therapeutic target through pharmacological inhibition by 5-(N-ethyl-N-isopropyl)-Amiloride (EIPA) or RNA interference.

Materials and methods

Cell line and reagents

A549 and H1299 non-small cell lung cancer (NSCLC) cells were cultured in Dulbecco's Modified Eagle Medium (DMEM, Gibco™, Waltham, MA, USA) supplemented with 10% fetal bovine serum (FBS, HyClone Laboratories Inc., South Logan, UT, USA), 1 mM sodium pyruvate (Gibco), 2 mM L-glutamine (Gibco), 100 µg/ml Penicillin/Streptomycin/Amphotericin B (Gibco), and 1X non-essential amino acids (Gibco) in a 37°C, 5% CO_2 incubator. Stable clones of BMI1-expressing cell lines were established as described in our previous work [17] and maintained as the condition of A549 cells, except for being selected with 20 µg/ml blasticidin S (TOKU-E, Bellingham, WA, USA). The NHE family inhibitor EIPA (5-(N-ethyl-N-isopropyl)-Amiloride) (Cat# 1154-25-2), obtained from Cayman Chemicals (Ann Arbor, MI, USA), was initially dissolved in dimethyl sulfoxide (DMSO) at a concentration of 20 mM and stored at -20°C. The pan-caspase inhibitor Z-VAD-FMK (Cat# FMK001), purchased from R&D Systems (Minneapolis, MN, USA), was dissolved in DMSO to yield a 20 mM stock solution and then stored at -20°C.

Analysis of The Cancer Genome Atlas (TCGA) data

Raw gene-level read counts of *SLC9A7* and *CD274* in the lung adenocarcinoma (LUAD) dataset of TCGA data were normalized using the transcripts per million (TPM) method and were retrieved from the OncoDB website (https://oncodb.org/index.html). Overall surviv-

al analysis of lung cancer patients was performed by setting the cutoff expression level of the *SLC9A7* gene at a value of 3.85 in fragments per kilobase per million, and data were retrieved from the Human Protein Atlas website (https://www.proteinatlas.org/).

Cell viability assay

A549 (2×10^3) and H1299 (1×10^3) cells were seeded in 96-well plates and treated with increasing concentrations of EIPA (0-80 μM) for 72 h. Cell viability was measured using the MTT assay as follows: MTT solution (Sigma-Aldrich, St. Louis, MO, USA) was added to each well at a final concentration of 500 μg/ml and incubated at 37°C for 2 h. After incubation, formazan crystals were dissolved in DMSO, and the absorbance was measured at 570 nm with a microplate reader.

Tumorsphere cultivation

Cells were suspended in Dulbecco's Modified Eagle Medium/Nutrient Mixture F-12 (DMEM/F-12, Gibco) medium supplemented with 1% methylcellulose, 0.4% bovine serum albumin (BSA, Gibco), 10 ng/ml epidermal growth factor (PeproTech, Inc., Rocky Hill, NJ, USA), 10 ng/ml basic fibroblast growth factor (PeproTech), 2.5 μg/ml insulin (Sigma-Aldrich), 0.5X B27 supplement (Gibco), 1 μg/ml hydrocortisone (Sigma-Aldrich), and 4 μg/ml heparin (Sigma-Aldrich). The cells were then seeded into low attachment 6-well plates (Greiner Bio-One GmbH, Kremsmünster, Austria) at a density of 5×10^3 cells/well. Tumorspheres with a diameter larger than 100 μm were counted and pictured under an inverted light microscope (AE30, Motic Incorporation Ltd., Hong Kong) on day 14.

Intracellular pH (pHi) measurement

Cells were seeded at a density of 1×10^4 cells per well in 96-well black plates and treated with EIPA (10 μM or 20 μM) for 24 h. pH measurement was conducted by using an intracellular pH assay kit (Cat# ab228552, Abcam, Cambridge, UK) according to the manufacturer's instructions. The culture medium was replaced with HHBS buffer (Gibco) containing BCFL, AM dye-loading solution, and the dye-loading plate was incubated at 37°C for 30 minutes, followed by an additional 30-minute incubation at room temperature. pH measurement was then assessed by monitoring the fluorescence at Ex/Em = 490/535 nm. A lower fluorescence count indicated a more basic condition for pHi.

Western blot analysis

Cells were lysed using NETN lysis buffer (150 mM NaCl, 20 mM Tris-HCl, pH 8.0, 0.5% NP-40, 1 mM EDTA) supplemented with a protease inhibitor cocktail and a phosphatase inhibitor cocktail. The total protein concentration in each sample was quantified using the Dual Range BCA Protein Assay Kit (Visual Protein, Energenesis Biomedical Co., Ltd., Taipei, Taiwan). Thirty μg of extracted proteins were separated using 8%-10% SDS-PAGE and transferred onto a PVDF membrane (Pall Corporation, Washington, NY, USA). After blocking with 10% skim milk in TBS-T buffer (20 mM Tris-HCl, 150 mM NaCl, 0.05% Tween-20) at room temperature for 1 h, the PVDF membrane was incubated with selected primary antibodies at 4°C overnight, followed by incubation with secondary antibodies conjugated with horseradish peroxidase (HRP) at room temperature for 1 h. The antibodies used in this study are listed in Table S1. The signals were then developed by incubation with the WesternBright™ ECL HRP substrate (Advansta Inc., San Jose, CA, USA) and captured with the Amersham™ Imager 680 imaging system (Thermo Fisher Scientific). Quantification was performed using the ImageJ software (version 1.53v, National Institutes of Health, Bethesda, MA, USA).

Fluorescence activated cell sorting (FACS) analysis

To determine the distribution of cells in the cell cycle, treatment with EIPA (10 μM or 20 μM) was carried out for 72 hours followed by detachment using trypsin/EDTA (Gibco). Subsequently, 2×10^5 cells were fixed with 70% ethanol/phosphate-buffered saline (PBS) solution at 4°C overnight. The fixed cells were then suspended in PBS containing 0.1% Triton X-100 (Sigma-Aldrich), 0.2 mg/ml RNase A (Sigma-Aldrich), and 20 μg/ml propidium iodide (Sigma-Aldrich) and incubated at room temperature for 30 minutes. The stained cell samples were analyzed using the FACS Canto II flow cytometer (BD Biosciences, Franklin Lakes, NJ, USA), and the data was analyzed with FlowJo software (BD Biosciences). To determine cell surface PD-L1

expression, NSCLC cells were dissociated using an enzyme-free dissociation solution and resuspended in FACS staining buffer (0.4% BSA/PBS containing 0.05% NaN3). The cells were then stained with PE- or APC-conjugated mouse monoclonal anti-PD-L1 antibodies (clone name: 29E.2A3, BioLegend, San Diego, CA, USA) at room temperature for 30 minutes. The fluorescence signals were detected using the FACS Canto II flow cytometer, and the data was analyzed using the FlowJo software.

RNA extraction and qRT-PCR

NSCLC cells were used to extract total RNA, using TRIzol™ Reagent (Invitrogen, Thermo Fisher Scientific). Two micrograms of total RNA were reverse-transcribed to complementary DNA (cDNA) using the RevertAid First Strand cDNA Synthesis Kit (Thermo Fisher Scientific). The Eco 48 real-time PCR system (PCRmax, Staffordshire, UK) was employed to perform quantitative RT-PCR with iQ™ SYBR® Green Supermix (Bio-Rad, Hercules, CA, USA) using the following primers: *SLC9A7*, 5'-CCTCATGTCCTGGAGCACGTTT-3' (forward) and 5'-GGTTCGACTTCTTGATTCCACCG-3' (reverse); *MRPL19*, 5'-GGGATTTGCATTCAGAGATCAG-3' (forward) and 5'-GGAAGGGCATCTCGTAAG-3' (reverse). The expression level of *SLC9A7* were normalized to that of *MRPL19* in the same sample, and the results were analyzed using the $2^{-\Delta\Delta Ct}$ method.

RNA interference

RNA interference technology was employed to knockdown NHE7. Gene-specific siRNA oligonucleotides against NHE7 (Cat# sc-62555) and control siRNA (Cat# No. sc-37007) were procured from Santa Cruz Biotechnology (Dallas, TX, USA). Cells were seeded at a density of 1×10^5 cells per well in 6-well plates and incubated for 24 h. Next, TransIT-X2:DNA complexes consisting of 50 nM or 100 nM siRNA and 7.5 µl TransIT-X2™ transfection reagent (Mirus Bio LCC, Madison, WI, USA) were formed in Opti-MEM medium (Gibco) and added to the wells. Cells were harvested at 48 h post-transfection for further experiments, and the knockdown efficiency was determined by qRT-PCR.

Preparation of nucleus/cytoplasm fractions

Isolation of nuclear and cytoplasmic fractions of cells was performed by using the Nuclear Protein Isolation-Translocation Assay Kit (Cat# NPI-1, FIVEphoton Biochemicals, San Diego, CA, USA) in accordance with the manufacturer's protocol. Lamin B1 and α-tubulin were used as loading controls for nuclear and cytoplasmic fractions, respectively.

Luciferase reporter assay

The STAT3 response element sequence (GTCGACATTTCCCGTAAATCGTCGA) [18] was synthesized as four repeats and was inserted into a pGL3-basic vector that contained the firefly luciferase reporter gene by using Kpn I and Bgl II cutting sites. To analyze STAT3 transcriptional activity, STAT3 reporter vector DNA was mixed at a ratio of 100:1 with a pRL-TK vector that contained the Renilla luciferase reporter gene (Promega Corporation, Madison, WI, USA), followed by complexing with TransIT-X2™ transfection reagent. After adding the DNA/transfection reagent complex for 48 hours, the cells were then lysed with passive lysis buffer (Promega). The activities of firefly and Renilla luciferases were measured using Dual-Luciferase® Reporter reagent (Promega) with a GloMax® 20/20 Luminometer (Promega).

Statistical analysis

Quantitative data were presented as mean ± SD from at least two independent experiments. Statistical analysis was performed using the Student's *t*-test for comparison between two groups and one-way ANOVA for comparison among multiple groups. Two-tailed *p*-values less than 0.05 were considered statistically significant for all tests.

Results

Inhibition of NHE activity by EIPA reduces cell proliferation and CSC activity in NSCLC cells

We first analyzed the differential expression levels of the *SLC9A7* gene between normal lung tissues and LUAD tissues in TCGA data and found that *SLC9A7* mRNA was significantly higher in LUAD tissues ($P < 0.0001$, **Figure 1A**). Kaplan-Meier survival curve analysis of LUAD patients in TCGA data was further performed using the median of *SLC9A7* mRNA expression as a cutoff, and it was found that LUAD patients with high expression of *SLC9A7* had a significantly lower overall survival than those with low expression of *SLC9A7* ($P = 0.007$, **Figure 1B**),

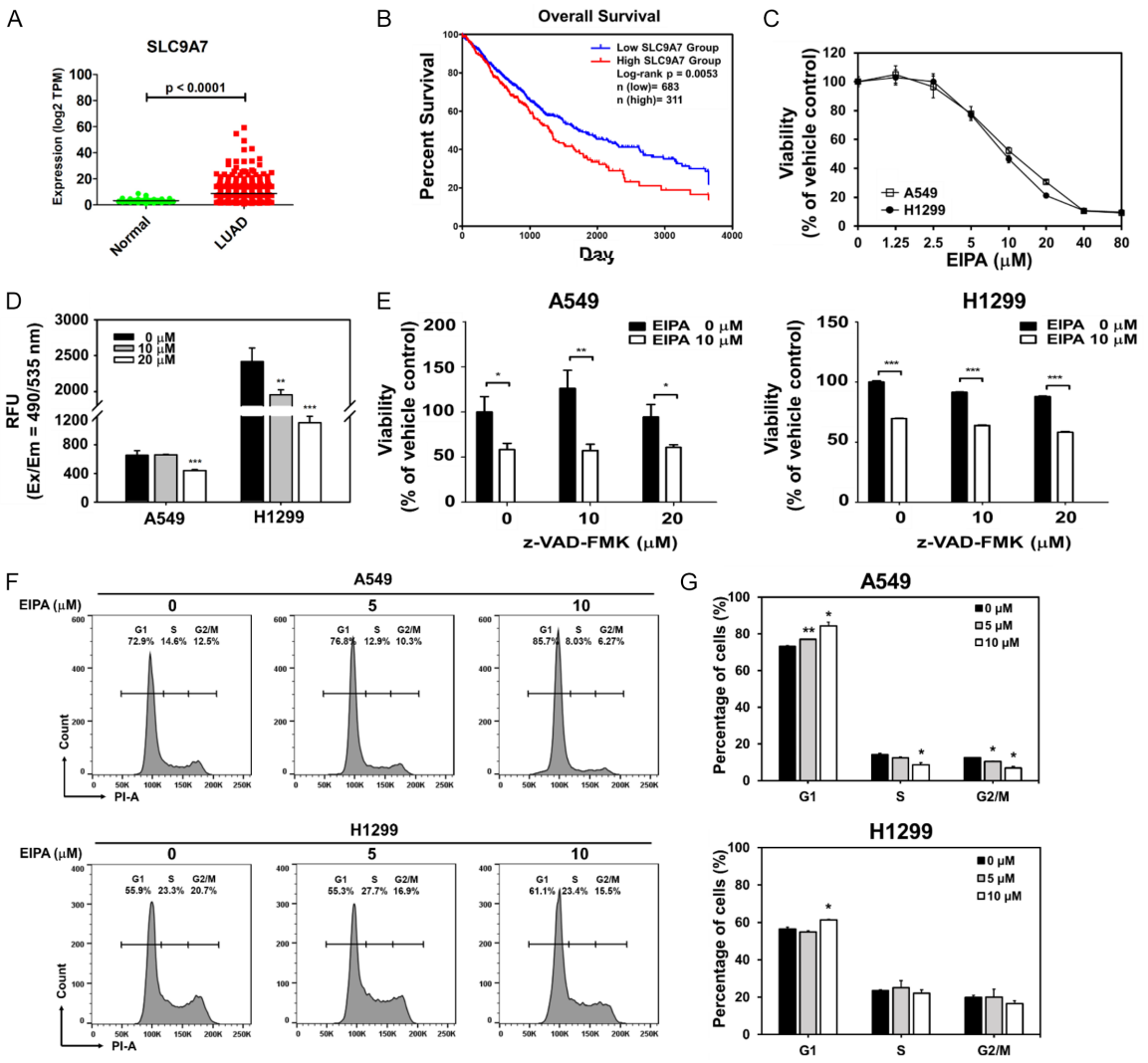

Figure 1. EIPA inhibits cell proliferation and cell cycle progression of NSCLC cells. (A, B) The differential expression levels of *SLC9A7* mRNA between normal and LUAD tissues and the correlation between *SLC9A7* mRNA expression levels and overall survival of lung cancer patients in the TCGA database were analyzed. (C) A549 and H1299 cells were seeded in 96-well plates and treated with a sequential concentration of EIPA for 72 h. Cell viability was determined using the MTT assay. (D) For pHi measurement, A549 and H1299 cells were seeded in 96-well black plates and treated with EIPA (10 μM or 20 μM) for 24 h. The cells were then stained with BCFL, AM dye for 1 h, followed by fluorescence signal detection (Ex/Em = 490/535 nm). (E) A549 and H1299 cells were treated with EIPA at a concentration of 10 μM for 72 h with AND without co-treatment with 10 μM or 20 μM of Z-VAD-FMK. Cell viability was determined using the MTT assay. *, $P < 0.05$; **, $P < 0.01$; ***, $P < 0.001$. (F, G) For cell cycle analysis, A549 and H1299 cells were treated with EIPA (10 μM or 20 μM) for 72 h and harvested for PI staining. The fluorescence signals were collected by flow cytometry and then analyzed with FlowJo software (F). The quantification results were calculated from two independent experiments (G). *, $P < 0.05$; **, $P < 0.01$.

indicating a positive correlation between *SLC9A7* and the severity of NSCLC. Then, we treated NSCLC cells with EIPA, a small molecule compound which has been used to inhibit NHE7 activity [19, 20], and observed its effect on cell proliferation. It was found that the proliferation of NSCLC cells, including A549 and H1299 cells, was inhibited with increasing EIPA concentration, and the IC_{50} was approximately 10 μM (**Figure 1C**). We also detected the intracellular pH (pHi) value of the A549 and H1299 cells after EIPA treatment and found that the fluorescence value decreased with increasing EIPA concentration, indicating that EIPA could indeed increase the pHi. However, the concentration required to make the alkalization of pHi

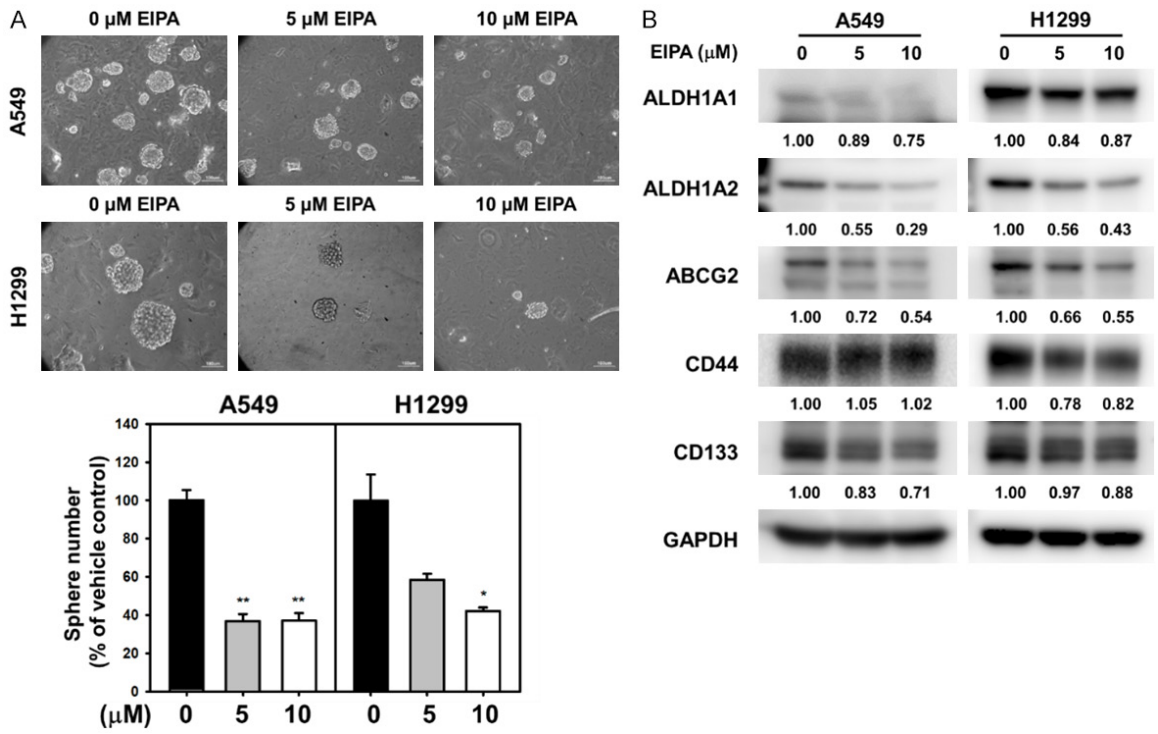

Figure 2. EIPA suppresses CSC activity in NSCLC cells. A. The CSC activities of A549 and H1299 cells were determined by tumorsphere cultivation. 5×10^3 cells were seeded into ultralow attachment 6-well plates under the treatment of indicated concentrations of EIPA. The formed tumorspheres were pictured and counted on day 14, and the inserted scale bars indicated 100 μm in length. *, $P < 0.05$; **, $P < 0.01$. B. The protein expression levels of lung CSC markers (ALDH1A1/ALDH1A2/ABCG2/CD44/CD133) were determined by western blot analysis. GAPDH was used as the loading control. The inserted numbers represented the relative expression levels compared to the vehicle control group (indicated as 0 μM).

was more than 20 μM (**Figure 1D**). With the treatment of z-VAD-FMK, a pan-caspase inhibitor, at concentrations of 10 μM or 20 μM, the growth inhibitory effect of EIPA at a concentration of 10 μM on NSCLC cells was not affected (**Figure 1E**), indicating that EIPA did not induce cell apoptosis to achieve the growth inhibitory effect on NSCLC cells. Cell cycle analysis with PI staining showed that, for both A549 and H1299 cells, the proportion of cells in the G1 phase was significantly increased when the EIPA concentration was increased to 10 μM (**Figure 1F** and **1G**), indicating that EIPA inhibited the proliferation of NSCLC cells by inducing G1 arrest. The effect of EIPA on CSC activity in NSCLC cells was assessed by tumorsphere cultivation. The results indicated that 10 μM of EIPA inhibited the number of tumorspheres in both A549 and H1299 NSCLC cells (**Figure 2A**). Furthermore, EIPA dose-dependently reduced the expression of several CSC marker proteins in both A549 and H1299 cells, such as ALDH1A2 and ABCG2 (**Figure 2B**). There was downregulation of CD44 and CD133 in H1299 and A549 cells, respectively (**Figure 2B**). These findings suggest that EIPA exhibits anti-NSCLC activity by suppressing cell proliferation and decreasing CSC activity.

NHE7 is involved in the PD-L1 expression in NSCLC cells, which links to the suppression of STAT3 activation

Due to the positive regulation role of PD-L1 in CSC activity [21], we hypothesized that NHE7 might be involved in PD-L1 expression in NSCLC cells. The correlation between the mRNA expression of *SLC9A7* (gene symbol for NHE7) and *CD274* (gene symbol for PD-L1) in the lung adenocarcinoma (LUAD) dataset of the TCGA database was examined by using the OncoDB webtool (https://oncodb.org/index.html), and a significantly positive correlation was found (**Figure 3A**). Using a median expression level as a cutoff, we also found significantly increased *CD274* mRNA in LUAD tissues with high *SLC9A7*

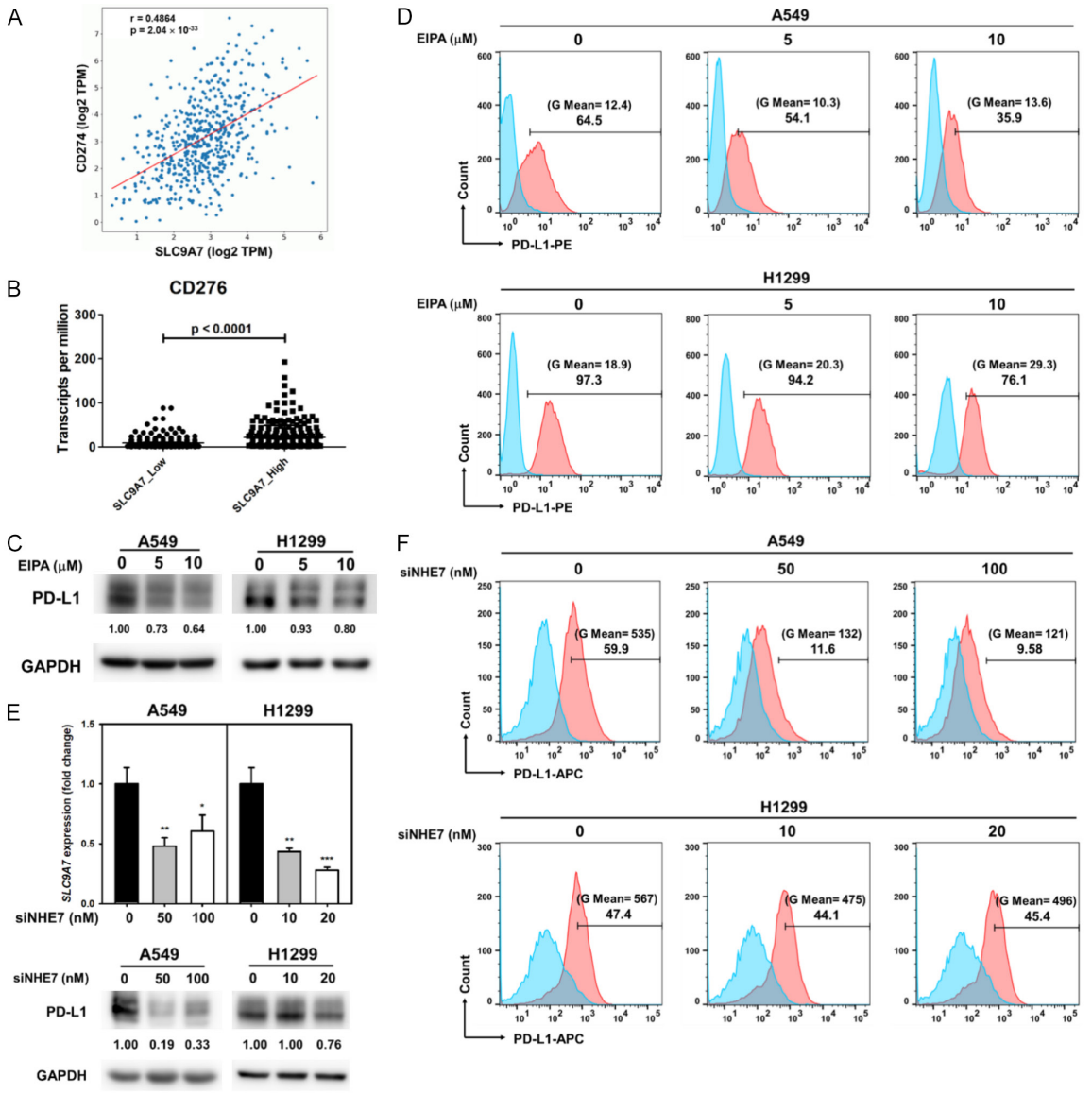

Figure 3. Inhibition of NHE7 expression or its activity decreases PD-L1 expression on NSCLC cells. (A, B) The mRNA expressions of *CD274* and *SLC9A7* in LUAD were obtained from the TCGA database. The correlation between mRNA expression of *SLC9A7* and *CD274* was analyzed using the OncoDB webtool (https://oncodb.org/index.html) (A). The LUAD subjects in the TCGA database were divided into two groups, SLC9A7_Low and SLC9A7_High, using the median expression level as a cutoff to compare the *CD274* mRNA levels (B). (C, D) The PD-L1 expression levels of A549 and H1299 cells under EIPA treatment were determined by western blot (C) and FACS (D) analyses. The inserted numbers in (C) represented the relative expression levels compared to the vehicle control group (indicated as 0 μM), after normalization to GAPDH. Blue peaks and red peaks in (D) represented an isotype control and an anti-PD-L1 antibody, respectively. (E, F) A549 and H1299 cells were transfected with NHE7-specific siRNA oligonucleotides (siNHE7) for 48 h, and the knockdown efficiency was determined by qRT-PCR (E). The PD-L1 expression levels were determined by western blot (E) and FACS (F) analyses. The inserted numbers in (E) represented the relative expression levels compared to the siNC group (indicated as 0 nM), after normalization to GAPDH. Blue peaks and red peaks in (F) represented an isotype control and an anti-PD-L1 antibody, respectively. siNC, negative control siRNA.

mRNA expression (**Figure 3B**, P < 0.0001). The treatment of EIPA in A549 and H1299 cells caused the downregulation of total PD-L1 protein expression (**Figure 3C**) and the positive percentage of membrane PD-L1 in a dose-dependent manner (**Figure 3D**). In addition to EIPA treatment, the knockdown of NHE7 by siRNA (**Figure 3E**, upper panel) also led to the suppression of total PD-L1 protein levels (**Figure 3E**, lower panel) in both A549 and

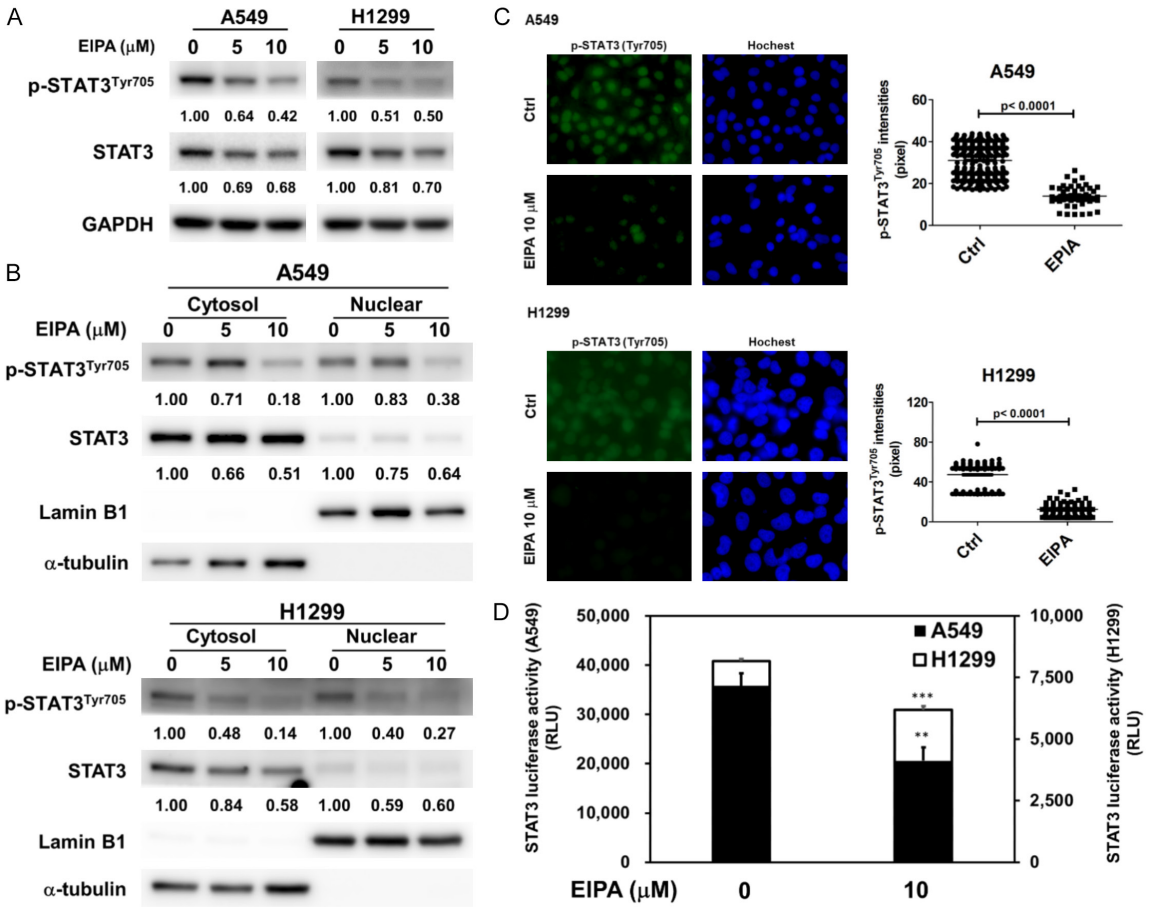

Figure 4. EIPA suppresses STAT3 activation in NSCLC cells. (A, B) Total cellular proteins (A) and the nuclear/cytoplasmic fractions (B) of A549 and H1299 cells under EIPA treatment were extracted and the protein expression levels of p-STAT3^{Tyr705} and STAT3 were determined by western blot analysis. GAPDH in (A) was used as the loading control. Lamin B1 and α-tubulin in (B) was used as the markers for nuclear and cytoplasmic proteins, respectively. The inserted numbers represented the relative expression levels compared to the vehicle control group (indicated as 0 μM). (C) A549 and H1299 cells were treated with 0.1% DMSO (ctrl) or 10 μM of EIPA for 72 hours, and the expressions of p-STAT3^{Tyr705} were examined by immunohistochemistry. The fluorescence intensities of p-STAT3^{Tyr705} were quantified from four independent fields by Image J software. (D) A549 and H1299 cells were transfected with 1 μg of luciferase-based STAT3 reporter plasmid for 24 hours and treated with 10 μM EIPA for a further 48 hours followed by determination of firefly luciferase activity from 100 μg of total cellular proteins. RLU, relative light unit. **, P < 0.01; ***, P < 0.001 after comparison to non-treated cells.

H1299 cells. Knockdown of NHE7 also displayed inhibitory effects in the membrane expression of PD-L1 in A549 cells (**Figure 3F**, upper panel) and the fluorescence intensity of the membrane PD-L1 staining level in H1299 cells (**Figure 3F**, lower panel). It has been reported that the inhibition of STAT3 activation could lead to a reduced PD-L1 level in cancer cells [22]. With western blot analysis, dose-dependent reductions in p-STAT3^{tyr705} by EIPA treatment was observed in both A549 and H1299 cells (**Figure 4A**). EIPA treatment displayed an inhibitory effect of the p-STAT3^{tyr705} protein level in cell nuclei when using cell fractionation extraction of cytoplasmic or nuclear proteins from A549 or H1299 cells followed by western blotting (**Figure 4B**). The reduced nuclear p-STAT3^{tyr705} levels in A549 and H1299 NSCLC cells were also confirmed by immunofluorescence staining (**Figure 4C**). In addition to nuclear expression of STAT3^{tyr705}, reductions in STAT3 transcriptional activity by EIPA treatment in A549 and H1299 NSCLC cells were also observed in a luciferase-based reporter assay (**Figure 4D**). These results present an inhibitory effect of EIPA in PD-L1 expression in NSCLC cells, which is associated with the suppression of STAT3 activation.

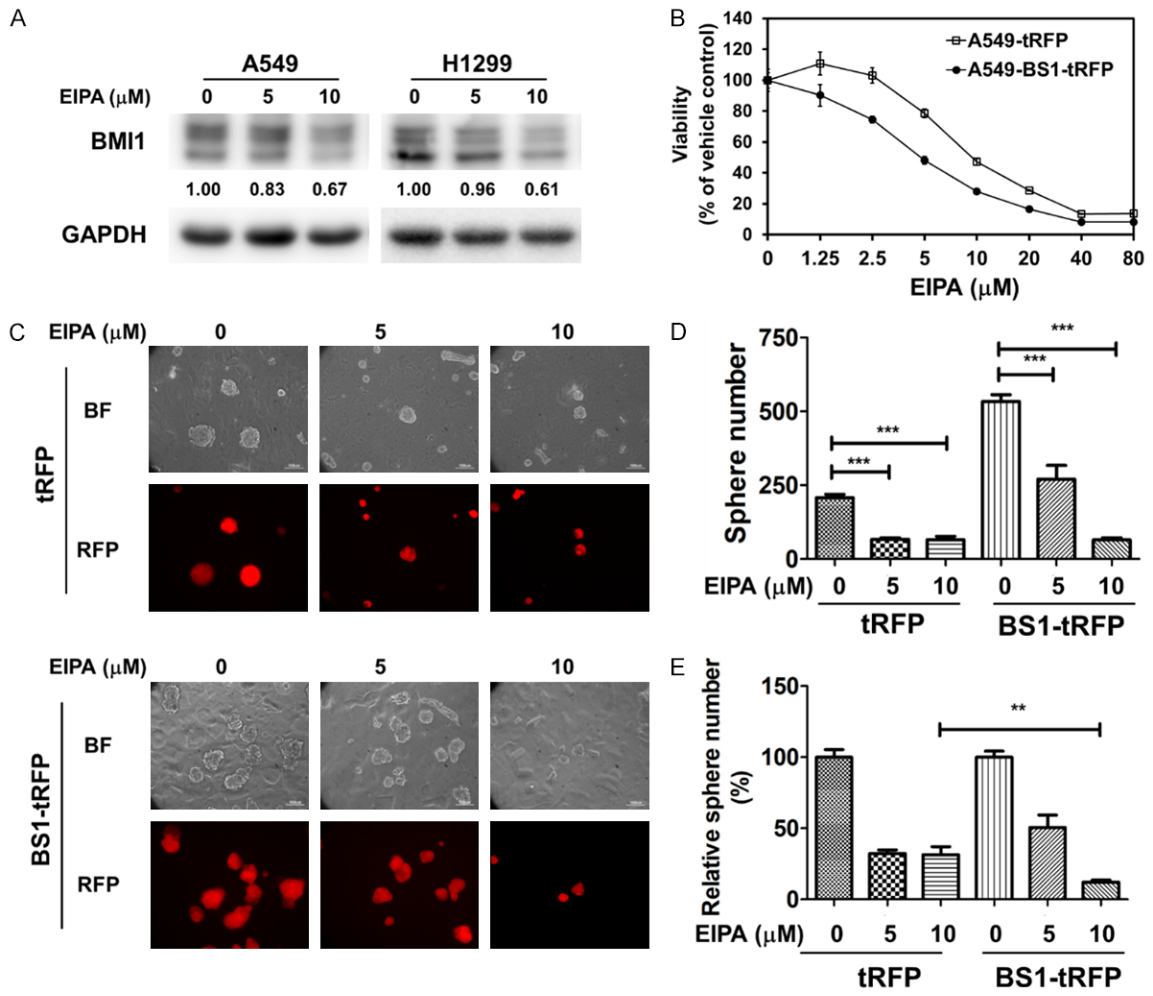

Figure 5. EIPA displays better CSC-targeting efficiency in BMI1-overexpressing NSCLC cells. (A) The BMI1 expression levels of A549 and H1299 cells under EIPA treatment were determined by western blot analysis. GAPDH was used as the loading control. The inserted numbers represented the relative expression levels compared to the vehicle control group (indicated as 0 μM). (B) A549 cells were transduced with lentiviruses of tRFP control (A549-tRFP) or flag-tagged-BMI1 (A549-BS1) and selected with 20 μg/ml blasticidin S. The cells were then seeded in 96-well plates and treated with a sequential concentration of EIPA for 72 h. Cell viability was determined using the MTT assay. (C-E) The CSC activities of A549-tRFP and A549-BS1 cells were assessed by tumorsphere cultivation. 5×10^3 cells were seeded into ultralow attachment 6-well plates under the treatment of indicated concentrations of EIPA. The formed tumorspheres were pictured and counted on day 14 (C). The inserted scale bars in (C) indicated 100 μm in length. BF, bright field; RFP, red fluorescent protein. The counted tumorsphere numbers were presented in (D). The relative sphere numbers after normalization to the untreated cells of each group were presented in (E). **, $P < 0.01$; ***, $P < 0.001$.

EIPA preferentially inhibits malignant phenotypes in BMI1-overexpressing NSCLC cells

We previously demonstrated that increased BMI1 expression was observed in pemetrexed-resistant A549 cells and the suppression of BMI1 activity reduced their CSC activity [23]. To explore the potential link between BMI1 expression and the inhibitory effect of EIPA in CSC activity, the BMI1 protein expression was examined and results revealed that EIPA treatment dose-dependently reduced the BMI1 protein level in both A549 and H1299 cells (**Figure 5A**). A better inhibitory effect of EIPA in cell proliferation was also observed in BMI1-overexpressing A549 cells (A549-BS1-tRFP, **Figure 5B**). The increased CSC activity with BMI1 overexpression was confirmed in A549-BS1-tRFP cells by tumorsphere cultivation (**Figure 5C** and **5D**). A greater suppression in tumorsphere formation by EIPA treatment was observed at a concentration of 10 μM (**Figure 5E**, decreased to 31.8% for A549-tRFP control cells but to 12.1% for A549-BS-tRFP cells when compared to

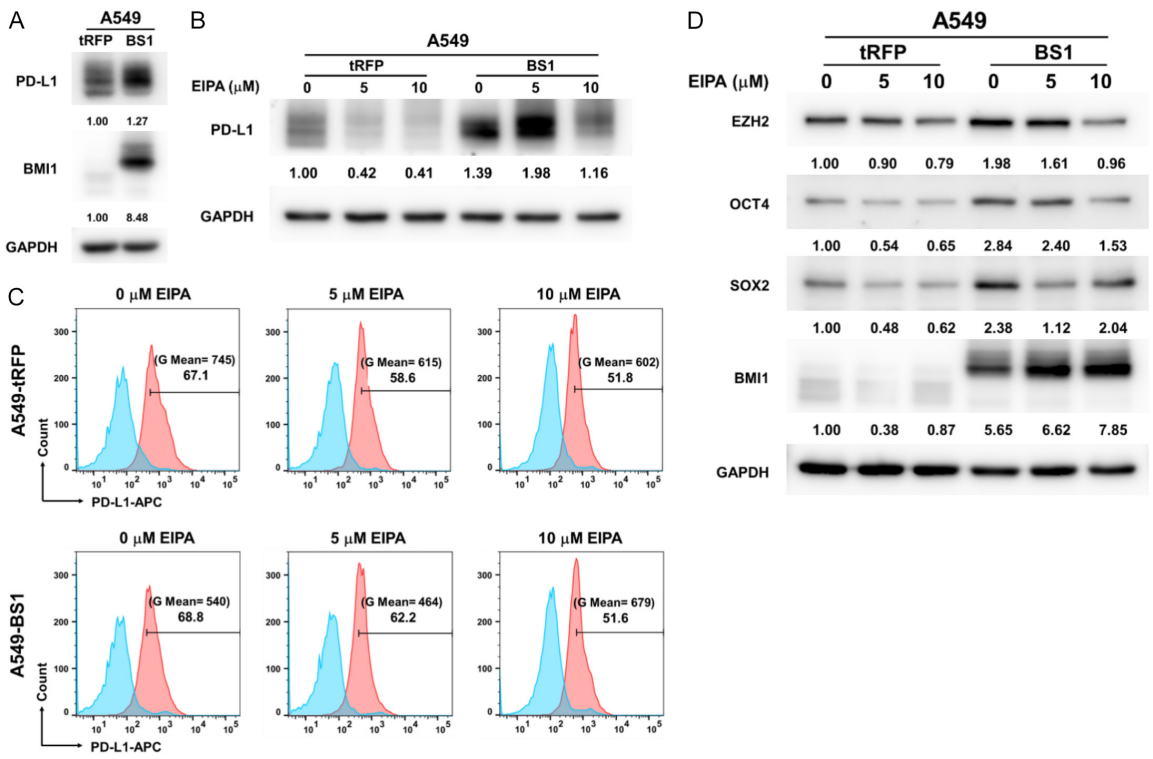

Figure 6. PD-L1 expression is increased in BMI1-overexpressing NSCLC cells. (A) The protein expression levels of BMI1 and PD-L1 in A549-tRFP and A549-BS1 cells were determined by western blot analysis. GAPDH was used as the loading control. The inserted numbers represented the relative expression levels compared to the A549-tRFP group, after normalization to GAPDH. (B-D) The expression levels of PD-L1 (B, C) and cancer stemness proteins (EZH2/OCT4/SOX2/BMI1) (D) in A549-tRFP and A549-BS1 cells were determined by western blot or FACS analysis. GAPDH was used as the loading control. The inserted numbers in (B) and (D) represented the relative expression levels compared to the vehicle control group (indicated as 0 μM). Blue peaks and red peaks in (C) represented an isotype control and an anti-PD-L1 antibody, respectively.

untreated counterpart cells). The increased PD-L1 expression in A549 cells was also observed after BMI1 overexpression (**Figure 6A**). Although EIPA reduced PD-L1 expression in A549-tRFP control cells at the total protein level (**Figure 6B**) and the membrane form (**Figure 6C**, upper panel), it increased the fluorescence intensities of PD-L1 staining in BMI1-overexpressing A549 cells (**Figure 6C**, lower panel), suggesting EIPA may increase PD-L1 expression on cell membranes in NSCLC cells with high BMI1 expression levels. We also examined the expression levels of cancer stemness factors in BMI1-overexpressing A549 cells under EIPA treatment, and results revealed that the increased EZH2, OCT4, and SOX2 in A549-BS1-tRFP cells could be reduced by EIPA (**Figure 6D**). These results indicate that EIPA preferentially inhibits cell proliferation and CSC activity in NSCLC cells with high BMI1 expression.

Discussion

NHEs have been associated with cell cycle progression and proliferation in various cancer types [24, 25]. Our study demonstrated that EIPA treatment disrupted cell cycle progression in NSCLC cells, which may be partly attributed to the inhibition of NHE7 activity. Using gene set enrichment analysis (GSEA) and the LUAD dataset of the TCGA database, an enrichment of the G2/M checkpoint signature was found in LUAD tissues with high expression of *SLC9A7* mRNA (Figure S1A). This finding supports the data of reduction of G2/M cells in EIPA-treated A549 cells (**Figure 1E**) and is similar to a previous report that NHE1 in breast cancer cells resulted in the delayed G2/M transition [26]. NHEs have been implicated in promoting tumor cell invasion and metastasis by regulating extracellular pH and intracellular signaling pathways. For example, NHE1 has been report-

ed to associate with epidermal growth factor (EGF) receptors to promote EGF-induced cell invasion in pancreatic cancer cells [27]. The overexpression of NHE7 in MDA-MB-231 breast cancer cells led to increased invasiveness in vitro and in vivo [15]. It has also been reported that NHE7 was colocalized with vimentin and actin in focal complexes using immunofluorescence staining in MDA-MB-231 cells, and vimentin directly interacted with NHE7 by co-immunoprecipitation [14]. Using GSEA of the TCGA data, we also found enrichment of EMT molecular signatures in LUAD tissues with high *SLC9A7* mRNA expression (Figure S1B). Further investigation is required to understand if NHE7 is involved in the invasiveness of NSCLC cells. It has been reported that the silencing of NHE1 in T-cell acute lymphoblastic leukemia cells sensitized cells to the chemotherapy drug doxorubicin [28]. CSCs are known to play a critical role in cancer drug resistance [29]. Our study showed that EIPA treatment suppressed CSC activity, which could potentially improve the sensitivity of NSCLC cells to other therapeutic agents.

Simultaneously, the increased PD-L1 expression in EIPA-treated BMI1-overexpressing NSCLC cells suggests a potential shift towards a "hotter" tumor microenvironment. Elevated PD-L1 levels in A549 cells could be observed by cisplatin treatment, and the combination of cisplatin and anti-PD-L1 antibodies displayed a better anti-tumor growth effect than single agent treatments [30]. However, it is essential to consider that increased PD-L1 expression might suppress anti-tumor immune responses by inhibiting T-cell activation [31]. A combination therapy approach may be advantageous to capitalize on the dual effects of EIPA in BMI1-overexpressing NSCLC cells. Combining EIPA with immune checkpoint inhibitors, such as anti-PD-L1 or anti-PD-1 antibodies, may counteract the immune suppression mediated by the increased PD-L1 expression and enhance the anti-tumor immune response. MLN4924, a small molecule inhibitor of NEDD8-activating enzyme, has been shown to induce PD-L1 expression on various cancer cells, including NSCLC cells, through mitogen-activated protein kinase kinase/c-Jun N-terminal kinase pathway [32]. The combination of the anti-PD-L1 antibody with MLN4924 achieved a significantly greater reduction of CT26 mouse colon cancer growth compared to treatment with only the anti-PD-L1 antibody [32]. Understanding the molecular mechanisms underlying the increased PD-L1 expression and the suppression of cancer stemness factors in response to EIPA treatment is crucial for optimizing therapeutic strategies. Identifying the signaling pathways and cellular processes involved could provide new insights into the complex relationship between cancer stem cells, immune checkpoint molecules, and the tumor microenvironment.

Acknowledgements

This work was supported by the National Science and Technology Council in Taiwan (grant Nos. 109-2314-B-371-010 and 110-2314-B-371-014 to B.Y.W.).

Disclosure of conflict of interest

None.

Address correspondence to: Dr. Wen-Wei Chang, Department of Biomedical Sciences, Chung Shan Medical University, No. 110, Sec. 1, Jianguo N. Rd., Taichung 402306, Taiwan. Tel: +886-4-24730022 Ext. 12305; Fax: +886-4-23248187; E-mail: changww@csmu.edu.tw

References

[1] Zou Z, Tao T, Li H and Zhu X. mTOR signaling pathway and mTOR inhibitors in cancer: progress and challenges. Cell Biosci 2020; 10: 31.

[2] Li C and Lu H. Adenosquamous carcinoma of the lung. Onco Targets Ther 2018; 11: 4829-4835.

[3] Tamura T, Kurishima K, Nakazawa K, Kagohashi K, Ishikawa H, Satoh H and Hizawa N. Specific organ metastases and survival in metastatic non-small-cell lung cancer. Mol Clin Oncol 2015; 3: 217-221.

[4] Brody R, Zhang Y, Ballas M, Siddiqui MK, Gupta P, Barker C, Midha A and Walker J. PD-L1 expression in advanced NSCLC: insights into risk stratification and treatment selection from a systematic literature review. Lung Cancer 2017; 112: 200-215.

[5] Doroshow DB, Sanmamed MF, Hastings K, Politi K, Rimm DL, Chen L, Melero I, Schalper KA and Herbst RS. Immunotherapy in non-small cell lung cancer: facts and hopes. Clin Cancer Res 2019; 25: 4592-4602.

[6] Ishibashi M, Tamura H, Sunakawa M, Kondo-Onodera A, Okuyama N, Hamada Y, Moriya K,

Choi I, Tamada K and Inokuchi K. Myeloma drug resistance induced by binding of myeloma B7-H1 (PD-L1) to PD-1. Cancer Immunol Res 2016; 4: 779-788.
[7] Gato-Canas M, Zuazo M, Arasanz H, Ibanez-Vea M, Lorenzo L, Fernandez-Hinojal G, Vera R, Smerdou C, Martisova E, Arozarena I, Wellbrock C, Llopiz D, Ruiz M, Sarobe P, Breckpot K, Kochan G and Escors D. PDL1 signals through conserved sequence motifs to overcome interferon-mediated cytotoxicity. Cell Rep 2017; 20: 1818-1829.
[8] Sato M, Harada-Shoji N, Toyohara T, Soga T, Itoh M, Miyashita M, Tada H, Amari M, Anzai N, Furumoto S, Abe T, Suzuki T, Ishida T and Sasano H. L-type amino acid transporter 1 is associated with chemoresistance in breast cancer via the promotion of amino acid metabolism. Sci Rep 2021; 11: 589.
[9] Yang L, Shi P, Zhao G, Xu J, Peng W, Zhang J, Zhang G, Wang X, Dong Z, Chen F and Cui H. Targeting cancer stem cell pathways for cancer therapy. Signal Transduct Target Ther 2020; 5: 8.
[10] Liberti MV and Locasale JW. The warburg effect: how does it benefit cancer cells? Trends Biochem Sci 2016; 41: 211-218.
[11] Pouyssegur J, Franchi A, L'Allemain G and Paris S. Cytoplasmic pH, a key determinant of growth factor-induced DNA synthesis in quiescent fibroblasts. FEBS Lett 1985; 190: 115-119.
[12] White KA, Grillo-Hill BK and Barber DL. Cancer cell behaviors mediated by dysregulated pH dynamics at a glance. J Cell Sci 2017; 130: 663-669.
[13] Numata M and Orlowski J. Molecular cloning and characterization of a novel (Na+,K+)/H+ exchanger localized to the trans-Golgi network. J Biol Chem 2001; 276: 17387-17394.
[14] Kagami T, Chen S, Memar P, Choi M, Foster LJ and Numata M. Identification and biochemical characterization of the SLC9A7 interactome. Mol Membr Biol 2008; 25: 436-447.
[15] Onishi I, Lin PJ, Numata Y, Austin P, Cipollone J, Roberge M, Roskelley CD and Numata M. Organellar (Na+, K+)/H+ exchanger NHE7 regulates cell adhesion, invasion and anchorage-independent growth of breast cancer MDA-MB-231 cells. Oncol Rep 2012; 27: 311-317.
[16] Galenkamp K, Jung M and Commisso C. pH homeostasis as a novel therapeutic target in pancreatic cancer. Pancreas 2019; 48: 1429-1430.
[17] Shen HT, Chien PJ, Chen SH, Sheu GT, Jan MS, Wang BY and Chang WW. BMI1-mediated pemetrexed resistance in non-small cell lung cancer cells is associated with increased SP1 activation and cancer stemness. Cancers (Basel) 2020; 12: 2069.
[18] Tsareva SA, Moriggl R, Corvinus FM, Wiederanders B, Schutz A, Kovacic B and Friedrich K. Signal transducer and activator of transcription 3 activation promotes invasive growth of colon carcinomas through matrix metalloproteinase induction. Neoplasia 2007; 9: 279-291.
[19] Galenkamp KMO, Sosicka P, Jung M, Recouvreux MV, Zhang Y, Moldenhauer MR, Brandi G, Freeze HH and Commisso C. Golgi acidification by NHE7 regulates cytosolic ph homeostasis in pancreatic cancer cells. Cancer Discov 2020; 10: 822-835.
[20] Milosavljevic N, Monet M, Lena I, Brau F, Lacas-Gervais S, Feliciangeli S, Counillon L and Poet M. The intracellular Na(+)/H(+) exchanger NHE7 effects a Na(+)-coupled, but not K(+)-coupled proton-loading mechanism in endocytosis. Cell Rep 2014; 7: 689-696.
[21] Liu YH, Li YL, Shen HT, Chien PJ, Sheu GT, Wang BY and Chang WW. L-type amino acid transporter 1 regulates cancer stemness and the expression of programmed cell death 1 ligand 1 in lung cancer cells. Int J Mol Sci 2021; 22: 10955.
[22] Jahangiri A, Dadmanesh M and Ghorban K. STAT3 inhibition reduced PD-L1 expression and enhanced antitumor immune responses. J Cell Physiol 2020; 235: 9457-9463.
[23] Shen HT, Chien PJ, Chen SH, Sheu GT, Jan MS, Wang BY and Chang WW. BMI1-mediated pemetrexed resistance in non-small cell lung cancer cells is associated with increased SP1 activation and cancer stemness. Cancers (Basel) 2020; 12: 2069.
[24] Horvat B, Taheri S and Salihagic A. Tumour cell proliferation is abolished by inhibitors of Na+/H+ and HCO3-/Cl- exchange. Eur J Cancer 1992; 29A: 132-137.
[25] Acevedo-Olvera LF, Diaz-Garcia H, Parra-Barrera A, Caceres-Perez AA, Gutierrez-Iglesias G, Rangel-Corona R and Caceres-Cortes JR. Inhibition of the Na+/H+ antiporter induces cell death in TF-1 erythroleukemia cells stimulated by the stem cell factor. Cytokine 2015; 75: 142-150.
[26] Flinck M, Kramer SH, Schnipper J, Andersen AP and Pedersen SF. The acid-base transport proteins NHE1 and NBCn1 regulate cell cycle progression in human breast cancer cells. Cell Cycle 2018; 17: 1056-1067.
[27] Cardone RA, Greco MR, Zeeberg K, Zaccagnino A, Saccomano M, Bellizzi A, Bruns P, Menga M, Pilarsky C, Schwab A, Alves F, Kalthoff H, Casavola V and Reshkin SJ. A novel NHE1-centered signaling cassette drives epidermal growth factor receptor-dependent pancreatic tumor metastasis and is a target for combination therapy. Neoplasia 2015; 17: 155-166.

[28] Altaf E, Huang X, Xiong J, Yang X, Deng X, Xiong M, Zhou L, Pan S, Yuan W, Li X, Hao L, Tembo KM, Xiao R and Zhang Q. NHE1 has a notable role in metastasis and drug resistance of T-cell acute lymphoblastic leukemia. Oncol Lett 2017; 14: 4256-4262.

[29] Zhou HM, Zhang JG, Zhang X and Li Q. Targeting cancer stem cells for reversing therapy resistance: mechanism, signaling, and prospective agents. Signal Transduct Target Ther 2021; 6: 62.

[30] Fournel L, Wu Z, Stadler N, Damotte D, Lococo F, Boulle G, Segal-Bendirdjian E, Bobbio A, Icard P, Tredaniel J, Alifano M and Forgez P. Cisplatin increases PD-L1 expression and optimizes immune check-point blockade in non-small cell lung cancer. Cancer Lett 2019; 464: 5-14.

[31] Pardoll DM. The blockade of immune checkpoints in cancer immunotherapy. Nat Rev Cancer 2012; 12: 252-264.

[32] Zhang S, You X, Xu T, Chen Q, Li H, Dou L, Sun Y, Xiong X, Meredith MA and Sun Y. PD-L1 induction via the MEK-JNK-AP1 axis by a neddylation inhibitor promotes cancer-associated immunosuppression. Cell Death Dis 2022; 13: 844.

Table S1. Antibody information used in this study

Target	Company	Catalog number
ALDH1A1	GeneTex International Corporation, Taiwan	gtx123973
ALDH1A2	Proteintech Group, USA	13951-1-AP
ABCG2	ABclonal Technology, USA	A5661
CD44	Proteintech Group, USA	15675-1-AP
CD133	GeneTex International Corporation, Taiwan	gtx102109b
PDL1	GeneTex International Corporation, Taiwan	gtx104763
p-STAT3 (Tyr705)	GeneTex International Corporation, Taiwan	gtx118000
STAT3	GeneTex International Corporation, Taiwan	gtx104616
BMI1	Cell Signaling Technology, USA	6964S
EZH2	BD Biosciences, USA	BD612667
Oct4	Proteintech Group, USA	11263-1-AP
SOX2	Cell Signaling Technology, USA	23064S
Lamin B1	GeneTex International Corporation, Taiwan	gtx103292
α-tubulin	Proteintech Group, USA	66031-1-Ig
GAPDH	GeneTex International Corporation, Taiwan	gtx100118
Goat Anti-Mouse IgG antibody (HRP)	GeneTex International Corporation, Taiwan	gtx213111-01
Goat Anti-Rabbit IgG antibody (HRP)	GeneTex International Corporation, Taiwan	gtx213110-01

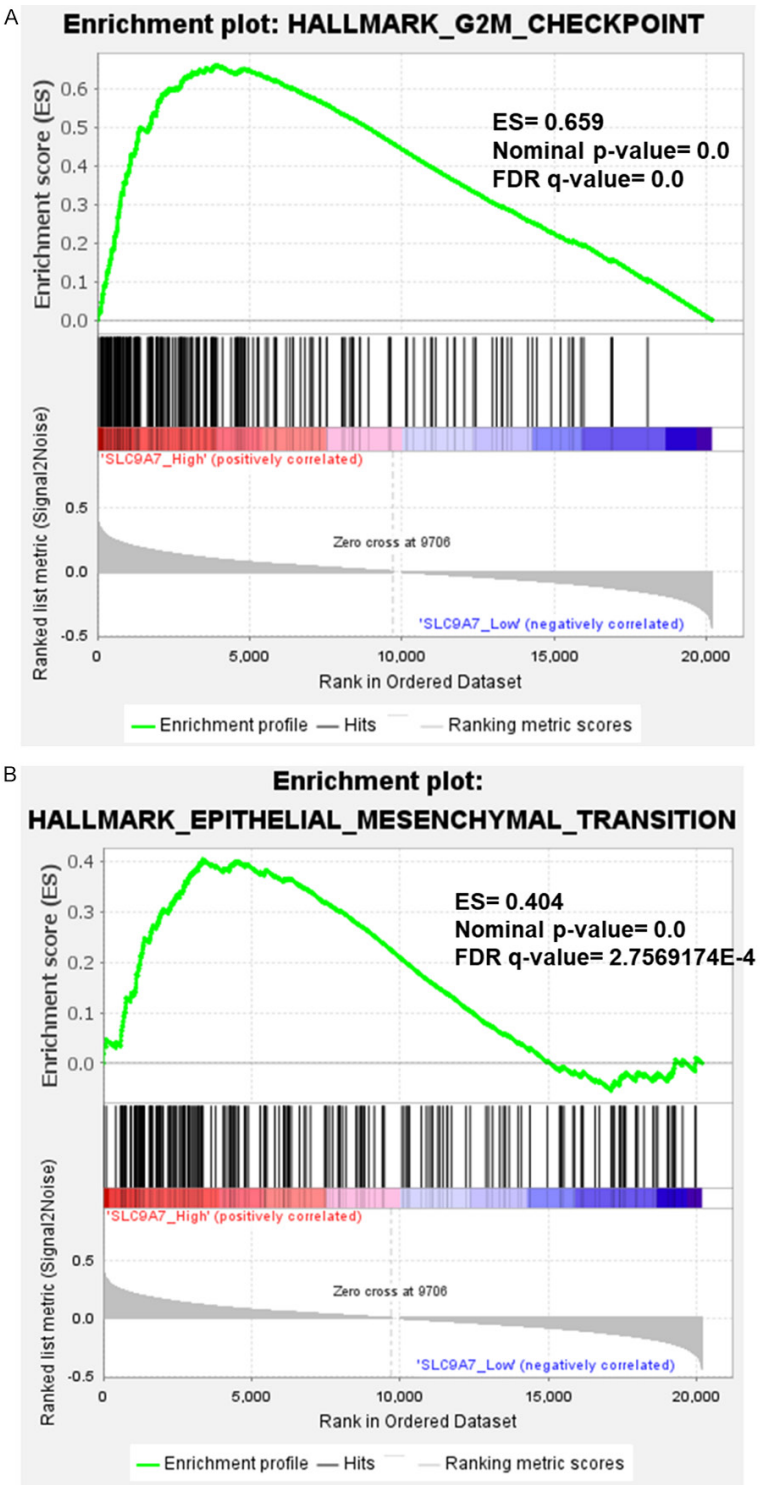

Figure S1. Gene set enrichment analysis of SLC9A7 mRNA expression level in NSCLC dataset of TCGA database. The median expression level of SLC7A7 mRNA was used as the cutoff-value for distinguishing low or high groups. Gene Set Enrichment Analysis was performed by GSEA software. A. Hallmark G2M checkpoint gene set; B. Hallmark Epithelial-mesenchymal transition gene set. ES, enrichment score. FDR, false discovery rate.